Eur Biophys J (1999) 28: 294–301 © Springer-Verlag 1999

ARTICLE

Paolo Mariani · Franco Rustichelli · Letizia Saturni
Lorenzo Cordone

Stabilization of the monoolein *Pn*3*m* cubic structure on trehalose glasses

Received: 5 October 1998 / Accepted: 13 November 1998

Abstract Trehalose is known to protect some organisms from various stresses due to drought and high temperature. To explore the molecular mechanism of the protective function, the mesomorphic properties of the monoolein-water system, dried in the presence of trehalose, were studied by X-ray diffraction. While, in pure water, two bicontinuous inverse cubic structures (the *Pn*3*m* and *Ia*3*d* phases) and a lamellar Lα phase exist as a function of concentration, only the *Pn*3*m* cubic phase has been detected in concentrated trehalose solutions or in trehalose glasses, even under extremely dry conditions. Depending on the sugar concentration, or after glass dehydration, the *Pn*3*m* cubic unit cell decreases to very low values, much below the smaller one observed in pure water. However, as no phase transitions occur, a simple osmotic mechanism can be excluded. An additional stabilization of the lipid phase, arising from interfacial free energy changes due to trehalose-water-lipid direct interactions, and large enough to affect the energetic balance between the *Pn*3*m* and the *Ia*3*d* cubic phases, evidently occurs. Moreover, no differences in the *Pn*3*m* cubic structure were observed when the sugar platelets convert to the glassy state; no apparent structural modifications that can be related to mechanical pressure exerted on the lipid phase have been detected.

Key words Lipid polymorphism · Cubic phases · X-ray diffraction · Dehydration stress · Trehalose protective function

P. Mariani (✉) · F. Rustichelli · L. Saturni
Istituto di Scienze Fisiche, Università di Ancona,
and INFM, Istituto Nazionale per la Fisica della Materia,
Via Ranieri 65, I-60131 Ancona, Italy
e-mail: mariani@popcsi.unian.it

L. Cordone
Dipartimento di Scienze Fisiche ed Astronomiche,
Università di Palermo and INFM,
Istituto Nazionale per la Fisica della Materia,
Via Archirafi, Palermo, Italy

Introduction

Like other sugars, trehalose has been found to have a protective function on some organisms against damage due to dehydration (Crowe et al. 1984). Several plant seeds, spores, and macrocysts, as well as some species of soil-dwelling animals, are in fact able to survive complete dehydration for many years in a state of suspended animation (the so-called anhydrobiotic state), and rapidly swell and resume metabolic activity when they come in contact with water. Survival on dehydration has been correlated with the intracellular synthesis of trehalose during desiccation, and its degradation after rehydration (Crowe et al. 1984; Green and Angell 1989; Takahashi et al. 1997). The role of sugars in anhydrobiosis has been explained by considering two different mechanisms. It has been suggested that, in the dehydrated state, sugar molecules act as substitutes for water molecules by forming hydrogen bonds with the hydrophilic surfaces of proteins or lipids in cell membranes (Crowe et al. 1987; Crowe and Crowe 1988). However, dehydrated sugar solutions convert to amorphous solids (glasses); more likely, this process can account for the prevention of potein denaturation and cell fusion, since both phenomena involve intra- and intermolecular motions which are fully hindered in the glassy state (Green and Angell 1989; Franks et al. 1991; Cordone et al. 1998).

Several papers report the stabilizing effects of trehalose on some lipid phases (Crowe and Crowe 1988; Koynova et al. 1989; Koynova and Caffrey 1994; Tsonev et al. 1994; Takahashi et al. 1997). In particular, in hydrated lipid phases, trehalose produces a reduction of the surface-per-polar head at the lipid-water interface, stabilizing structures with low surface area (like inverted hexagonal phases), or inducing transitions from structures with higher to structures with lower interfacial area (for example, from lamellar Lβ to Lβ' phases). These changes in structural properties and in phase transition temperatures have been interpreted as a manifestation of the Hofmeister effect, in which the sugar acts as a kosmotropic reagent, stabilizing the structure of the water (Sanderson et al. 1991).

In order to explore the protective effect of trehalose under anhydrous conditions, we analyzed by X-ray diffraction the structural properties of the monoolein-water system, dried in the presence of trehalose. Monoolein in water shows, as a function of temperature and concentration, a crystalline lamellar phase Lc and several mesophases, characterized by a highly disordered conformation of the hydrocarbon chains (Hyde et al. 1984; Mariani et al. 1988; Briggs et al. 1996). In particular, a lamellar structure Lα, where lipid molecules assemble into stacked sheets, an inverted hexagonal phase H_{II}, which consists of cylindrical structure elements packed on a 2-D hexagonal lattice, and two inverted (type II) cubic phases with space group *Pn*3*m* (Q^{224}) and *Ia*3*d* (Q^{230}) have been identified (Longley and McIntosh 1983; Hyde et al. 1984; Mariani et al. 1988). The two cubic phases may be described in terms of infinite periodic minimal surfaces (IPMS), i.e., infinite arrays of connected saddle surfaces with zero mean curvature at each point (Scriven 1976). In these structures, lipid monolayers are draped across either side of the IPMS, touching it with their terminal methyl groups; this results in a 3-D periodic bicontinuous structure, formed by distinct water and lipid volumes. The crystallographic space group of the cubic phase determines the type of the IPMS; in particular, the inverse cubic phases observed in the monoolein-water system (space groups *Ia*3*d* and *Pn*3*m*) are based on the G (gyroid) and D (diamond) surfaces, respectively (Schoen 1970; Longley and McIntosh 1983; Mariani et al. 1988; Luzzati et al. 1993).

Materials and methods

D-(+)-Trehalose dihydrate and the monoacylglyceride 1-monoolein were obtained from Sigma (Milan, Italy) with purity of >99% and used without further purification.

The phase diagram of the trehalose-water system is shown in Fig. 1 (Green and Angell 1989); note that concentrations are here expressed as a water-to-trehalose molar ratio, n_{wat}/n_{tre}. Aqueous solutions of trehalose can, on dehydration or cooling, form amorphous solids (glasses). On heating, a classical glass transition, from the glassy to the so-called viscous-elastic rubbery state, is observed; as in other carbohydrate-water mixtures, the glass-transition temperature [i.e. the temperature at which molecular diffusion becomes observable on the differential scanning calorimeter time scale (seconds) and the liquid-like degrees of freedom become accessible] increases as the water content is reduced. Noticeable is the fact that for concentrations lower than about two molecules of water per molecule of trehalose the glassy state exists at room temperature. The phase diagram of the monoolein-water system is shown in Fig. 2 (Hyde et al. 1984; Mariani et al. 1988; Briggs et al. 1996); here the concentration is expressed as the weight of lipid per weight of mixture (c_{lip}). Note that the cubic *Pn*3*m* phase forms at room temperature in excess of water, and transforms into the

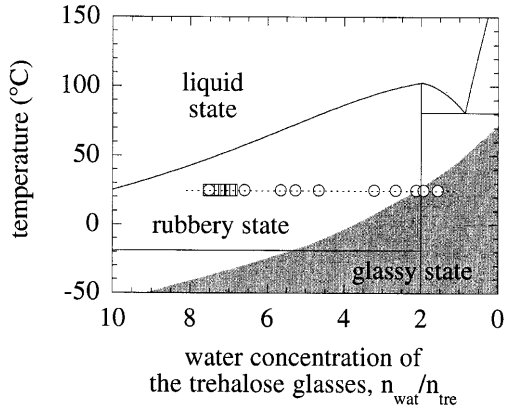

Fig. 1 Phase diagram of the trehalose-water system [redrawn from Green and Angel (1989)]. The water composition of the mixtures is reported as a molar ratio between water (wat) and trehalose (tre). The compound forming at $(n_{wat}/n_{tre})=2$ is therefore the trehalose dihydrate. The glassy state region is shown in *gray*. *Open squares* and *circles* indicate the concentration of trehalose glasses obtained by dehydrating lipid-containing trehalose solutions in the desiccator and in the 80 °C oven, respectively

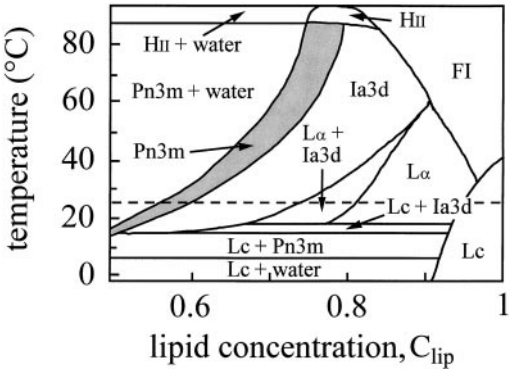

Fig. 2 Phase diagram of the monoolein-water system [redrawn from Briggs et al. (1996)]. The composition is expressed as weight of lipid per weight of mixture. Phases are labeled as in the text; *FI* stands for fluid isotropic. The *Pn*3*m* cubic phase region is shown in *gray*. The *dashed line* indicates the temperature at which experiments in pure water have been performed

*Ia*3*d* phase when the lipid concentration increases to about 0.65.

Mixtures containing monoolein in a vast excess of aqueous solutions of trehalose at different concentrations (from 0 to 2.5 M) were prepared and equilibrated for one day at room temperature. The lipid phase, which separates from the solution, was analyzed (1) in pure water, as a function of concentration [see also results reported by Mariani et al. (1988) and by Briggs et al. (1996)], (2) in excess trehalose solutions, as a function of the sugar concentration, and (3) completely embedded in anhydrous trehalose platelets, as a function of dehydration time. In the last case, monoolein-containing trehalose platelets were obtained by covering the lipid phase with a solution containing 80 mg trehalose per ml bidistilled water (0.2 M) and dehydrating the

samples for several hours in a silica-gel desiccator at 20 °C or in a 80 °C thermostatic oven. The final water concentration of the trehalose platelets was estimated by comparing the glass transition temperature, measured by differential scanning calorimetry, with those obtained from pure trehalose-dehydrated samples (Green and Angell 1989). The estimated concentration of the lipid-containing glasses is marked in the trehalose-water phase diagram shown in Fig. 1.

Diffraction measurements were carried out using two Philips PW1830 X-ray generators (Monza, Italy), both equipped with Guinier-type focusing cameras operating with bent crystal monochromators. Diffraction patterns were recorded in vacuo on a stack of four Kodak DEF-392 films or in air with a bent position-sensitive detector (INEL CPS120, France). Lipid samples and monoolein-containing trehalose platelets were mounted in vacuum-tight cells with thin mica windows.

Diffraction data were collected at 25 °C and analyzed following the usual procedure (Mariani et al. 1988). In each experiment a number of sharp low-angle reflections were observed and their spacings measured. The diffraction peaks were then indexed using equations which define the spacings of reflections for the different symmetry systems usually observed in lipid phases (lamellar, hexagonal, or *Pn*3*m*/*Ia*3*d*/*Im*3*m* cubic lattices); this problem was easy to solve, because in no case were extra peaks observed, which could be ascribed to the presence of other phases or to sugar crystallization. Moreover, in all the cases discussed in this paper a diffuse band observed in the $(3–5\ \text{Å})^{-1}$ region of the X-ray spectrum indicates the disordered (type α) nature of the lipid short-range conformation. Once the symmetry of the lipid phase was found, the dimensions of the unit cell were calculated. In the following, *a* indicates the unit cell dimension.

Results

Selected low-angle X-ray diffraction patterns, showing a number of reflections, are given in Fig. 3. By analyzing the spacing ratios of the low-angle diffraction peaks, the lipid phase has been identified (Mariani et al. 1988). While present X-ray data confirm the phase sequence previously reported for monoolein in pure water (Hyde et al. 1984; Mariani et al. 1988; Briggs et al. 1996), we observe that the *Pn*3*m* cubic phase exists in excess water at all the trehalose concentrations investigated, and also on trehalose platelets for all values of the dehydration times considered. Moreover, in trehalose platelets, in no case do extra peaks occur which can be ascribed to sugar crystallization; the trehalose is in an amorphous state at all the investigated dehydration conditions.

Some X-ray diffraction experiments have been also performed as a function of temperature. Both on monoolein samples prepared in excess of trehalose solutions or on trehalose dehydrated glasses, only the *Pn*3*m* cubic to H_{II} hexagonal phase transition has been detected on increasing the temperature. Moreover, the phase transition temperature

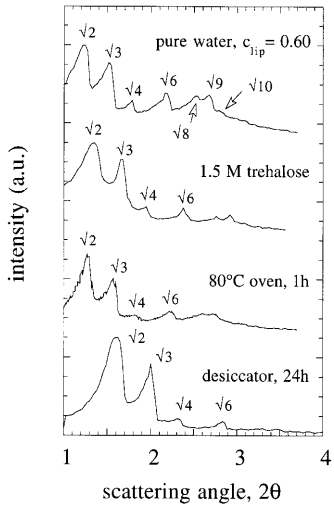

Fig. 3 Low-angle X-ray diffraction profiles obtained from monoolein in the different analyzed conditions. *From the top:* monoolein in pure water, $c_{lip} = 0.60$; monoolein in excess of 1.5 M trehalose aqueous solution; monoolein embedded in a trehalose glass dehydrated for 1 h in the 80 °C oven; monoolein embedded in a trehalose glass dehydrated for 24 h in the desiccator at 25 °C. Peaks are indexed according to the *Pn*3*m* space group (Mariani et al. 1988)

strongly depends on the trehalose concentration, decreasing from about 90 °C (observed in pure water excess) to 60 °C, observed in 2.5 M trehalose solution, and to 50 °C, observed in a trehalose glass with $n_{wat}/n_{tre} = 7$. In this last case the coincidence between the temperature of the *Pn*3*m*-H_{II} phase transition and the temperature of the transition from the rubbery to the liquid state observed in the trehalose-water system (see the phase diagram in Fig. 1) should be noted. Similar effects of stabilization of the hexagonal H_{II} phase at the expense of lamellar phases have been already observed in several other lipid systems in the presence of trehalose (Crowe et al. 1984; Koynova et al. 1989).

Monoolein in pure water

In pure water, the unit cell dimension of the different phases depends on concentration. The variations, observed both in the *Pn*3*m* and *Ia*3*d* cubic phases, are reported in the upper frame of Fig. 4. Given the assumption of distinct water and lipid regions within the unit cell, several structural parameters, which characterize the bicontinuous cubic phases, can be extracted from the cell dimension and sample concentration (Mariani et al. 1988; Turner et al. 1992; Briggs et al. 1996).

According to the IPMS model for the cubic phases, the lipid length L_{lip} can be calculated by solving the following equation (Turner et al. 1992):

$$c_{v,\,lip} = 2A_0(L_{lip}/a) + 4\pi/3\chi(L_{lip}/a)^3 \qquad (1)$$

where $c_{v,\,lip}$ is the lipid volume fraction, calculated from the composition of the lipid phase using $v_{lip} = 1.062\ \text{cm}^3\ \text{g}^{-1}$ (Lide 1996), and $v_{wat} = 1.0\ \text{cm}^3\ \text{g}^{-1}$ as specific volumes;

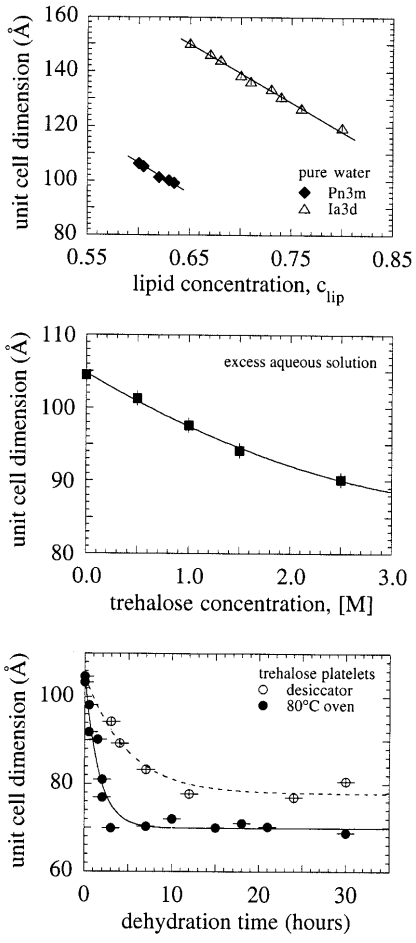

Fig. 4 Unit cell parameters of the cubic phases obtained in the different analyzed conditions. *Upper frame:* variation of the unit cell of the *Pn*3*m* and *Ia*3*d* cubic phases obtained in pure water as a function of concentration. *Lines* are guides to show the general trend. *Middle frame:* variation of unit cell of the *Pn*3*m* cubic phase obtained in excess of trehalose aqueous solution as a function of the sugar molar concentration. The *line* is a visual guide. *Lower frame:* variation of the unit cell of the *Pn*3*m* cubic phase obtained in trehalose glasses as a function of the dehydration times both in desiccator and in the 80 °C oven. The *lines* are the best exponential fits to the data (see text)

A_0 and χ are the constants for the minimal surface and have values specific to the different bicontinuous cubic phases (*Ia*3*d:* $A_0 = 3.091$, $\chi = -8$; *Pn*3*m:* $A_0 = 1.919$, $\chi = -2$) (Anderson et al. 1988). Note that in this model L_{lip} corresponds to the constant lipid monolayer thickness. The area-per-lipid at the headgroup a_0, i.e. at the water-lipid interface, can be then obtained using:

$$a_0 = 2A_L/n_{lip} \tag{2}$$

where

$$A_L = (A_0\, a^2 + 2\pi\chi\, L^2) \tag{3}$$

with $L = L_{lip}$, is the area at the headgroup integrated over a single monolayer and $n_{lip} = (c_{v,\,lip}\, a^3)/V_{lip}$ is the number of monoolein molecules (of molecular volume $V_{lip} = 629$ Å^3) contained in the unit cell. Finally, the mean curvature at the headgroup, averaged over the unit cell, $\langle H \rangle$, can be calculated by (Anderson et al. 1988):

$$\langle H \rangle = -2\pi\chi\, L/A_L \tag{4}$$

with $L = L_{lip}$. The sign of the curvature is positive, according to the fact that monoolein in water forms type II phases; practically, this means that the cross-sectional area per lipid decreases from the tail to the head, reducing to zero at the center of the water channel. It should be noticed that the area-per-lipid and mean curvature can be evaluated at any distance from the minimal surface by adjusting the value of L in Eqs. (3) and (4). For bicontinuous cubic phases, Caffrey and coworkers (Briggs et al. 1996) have shown that solving Eq. (3) under the condition that the cross-sectional area is zero, i.e. at a distance $L = L_{lip} + R_{wat}$ from the minimal surface, the radius R_{wat} of the water channel can be estimated. By making the appropriate substitutions, it follows:

$$R_{wat} = 0.391\, a - L_{lip} \tag{5}$$

and

$$R_{wat} = 0.248\, a - L_{lip} \tag{6}$$

for the *Pn*3*m* and *Ia*3*d* cubic phases, respectively.

As an alternative method, the structural parameters can also be calculated using a geometric approach (Gulik et al. 1985; Mariani et al. 1988; Luzzati et al. 1993). In this case the structure of the two bicontinuous cubic phases is described as being formed by networks of a number n of water-filled rods of radius R_{wat} and finite length λ (*Pn*3*m:* $n = 4$ and $\lambda = a\sqrt{3/2}$; *Ia*3*d:* $n = 24$ and $\lambda = a\sqrt{8}$). The expressions for the rod volume, ϕ, and surface, σ, with account being taken of the bevel-shaped junctions of the rods, are:

$$\phi = \pi R_{wat}^2\, \lambda\, (1 - k_v R_{wat}/\lambda) \tag{7}$$

and

$$\sigma = 2\pi R_{wat}\, \lambda\, (1 - k_s R_{wat}/\lambda) \tag{8}$$

where k_v and k_s are constants whose values are specific to the cubic phase (*Pn*3*m:* $k_v = 0.780$, $k_s = 1.068$; *Ia*3*d:* $k_v = 0.491$, $k_s = 0.735$). Therefore, from the composition and lattice parameter of the cubic unit cell, the rod volume can be estimated using $\phi = (1 - c_{v,\,lip})\, a/n$. Solving Eqs. (7) and (8), the radius of the water channels (R_{wat}) as well as the area-per-lipid ($a_0 = \sigma n/n_{lip}$) at the water-lipid interface can be finally calculated.

In Fig. 5 the monolayer thickness (L_{lip}), the area-per-lipid (a_0), the average over the unit cell of the mean curvature ($\langle H \rangle$) at the water-lipid interface, and the radius of the water channels (R_{wat}) are shown as a function of water concentration. The area-per-lipid at the headgroup and the radius of the water channels have been calculated using both IPMS and geometric approaches. According to previous results (see, in particular, Briggs et al. 1996), these parameters differ by only a few percent. However, in the case of the water channel radii, the assumption that the center of the water channel runs parallel to the minimal surface gives a systematic error in the calculations (see also

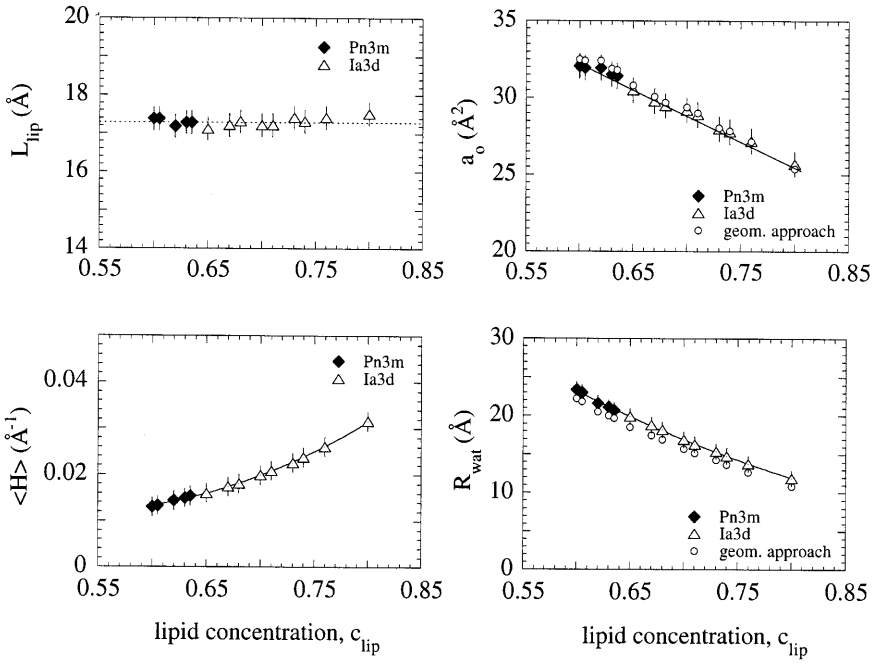

Fig. 5 Variation of the structural parameters of the *Pn*3*m* and *Ia*3*d* cubic phases obtained in pure water as a function of concentration. L_{lip} is the thickness of the lipid monolayer, i.e., the monoolein length; a_0 is the area-per-lipid at the headgroup; $\langle H \rangle$ is the average over the unit cell of the mean curvature calculated at the water-lipid interface; R_{wat} is the radius of the water channels. In the first (*left, upper side*) frame, the *horizontal dotted line* corresponds to a constant lipid length of 17.3 Å, calculated as reported by Caffrey and coworkers for monoolein at 25 °C (Briggs et al. 1996). In the other frames, continuous lines are visual guides to show the general trend. The *open circles* reported in the a_0 and R_{wat} plots (*right, upper* and *lower side*, respectively) indicate the corresponding values calculated using the geometric approach (see text)

Briggs et al. 1996), which results in a value of R_{wat} larger (by no more than about 1 Å) than the one calculated from the geometric approach. This is an important point: the R_{wat} values obtained from Eqs. (5) and (6) are estimates, but they define the upper limit of the water channel dimensions.

The data reported in Fig. 5 are in excellent agreement with previous analyses on the monoolein-water system (Longley and McIntosh 1983; Mariani et al. 1988; Briggs et al. 1996). While the lipid length remains practically constant (between 17 Å and 18 Å), the radius of the water channels decreases by reducing the water concentration; lower limits are about 20 Å in the *Pn*3*m* phase ($c_{lip} = 0.65$) and about 12 Å in the *Ia*3*d* phase ($c_{lip} = 0.80$). On further reducing the water content, the transition to the lamellar $L\alpha$ phase occurs. Moreover, as the water concentration decreases, the area-per-lipid at the water-lipid interface reduces continuously from about 33 Å^2 to 31 Å^2 and from 31 Å^2 to 26 Å^2 in the *Pn*3*m* and *Ia*3*d* cubic phases, respectively. It can be noted that an area-per-lipid of about 25 Å^2 has been observed on a monoolein monolayer at the air-water interface at the collapse pressure (Lide 1996).

A main result presented above should be stressed: the lipid length appears independent of composition and cubic phase type. As previously shown (Turner et al. 1992; Briggs and Caffrey 1994; Chung and Caffrey 1994; Briggs et al. 1996), L_{lip} is only dependent on temperature. For monoolein, the lipid length at 25 °C is expected to be 17.3 Å (Briggs et al. 1996). Then, along with the lattice parameters, the expected lipid length can be used to calculate by Eq. (1) the lipid concentration of the cubic phase, and by Eqs. (5) and (6) to estimate the radius of the aqueous channels.

Monoolein in excess of trehalose solutions

In excess aqueous solution, monoolein still forms the *Pn*3*m* cubic phase at all the concentrations of trehalose investigated. However, Fig. 4 (middle frame) shows that the unit cell strongly depends on the sugar concentration. Trehalose leads to a reduction of the cell dimension up to $a = 90$ Å, largely below the limit value observed in pure water.

Because the phase composition is unknown, to calculate the structural parameters of the *Pn*3*m* phase, the cell dimensions have been converted into lipid concentrations as indicated above, i.e. solving Eq. (1) under the assumption that L_{lip} is also independent of trehalose concentration. The lipid concentration in the *Pn*3*m* phase obtained using $L_{lip} = 17.3$ Å and the structural parameters calculated using Eqs. (2), (4), and (5) are then shown in Fig. 6 as a function of the trehalose concentration of the solution. It should be noted that in this case the aqueous medium contains sugar molecules (even if we continue to refer to it as "water"). In the calculations, however, no assumptions about the trehalose content of the lipid phase are made, so that the structural parameters obtained should reflect the lipid-water-sugar interactions.

The comparison with the structural parameters measured in pure water (Fig. 5) indicates that the *Pn*3*m* structure which forms in concentrated trehalose solutions is in an energetically unfavorable condition. The cubic phase shows highly curved monolayers ($\langle H \rangle = 0.020$ Å^{-1} compared to the value of 0.016 Å^{-1} observed in cubic *Pn*3*m* in pure water just before the phase transition to the *Ia*3*d* phase) and a rather small area-per-molecule at the water-lipid interface (30 Å^2 compared to 32 Å^2 observed in pure water just before the phase transition).

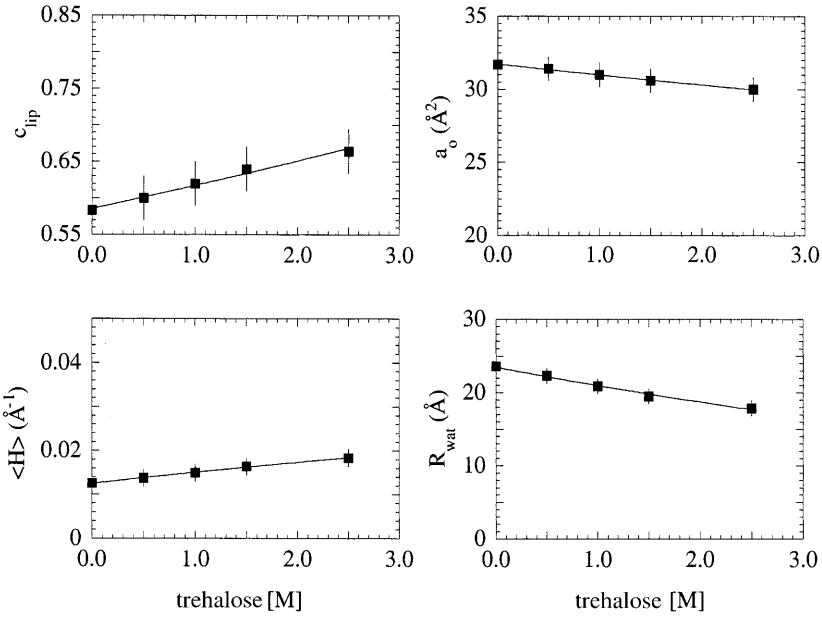

Fig. 6 Variation of the structural parameters of the *Pn*3*m* cubic phase obtained in excess of trehalose aqueous solution as a function of the sugar molar concentration. c_{lip} is the estimated lipid concentration of the cubic phase calculated as reported in the text assuming a constant lipid length for monoolein of 17.3 Å. Other notations and symbols as in the text and in Fig. 5. Lines are visual guides to show the general trend

Since it is exerted in excess water, the strong effect of trehalose on the structural properties of the *Pn*3*m* cubic phase might involve indirect (kosmotropic) interactions (Sanderson et al. 1991). However, as the structural parameters reach unusual values and no phase transitions occur, a simple osmotic mechanism can be excluded; an additional stabilization of the lipid phase, arising from interfacial free energy changes due to trehalose-water-lipid direct interactions, evidently occurs. Although reliable theoretical estimates of the free energy involved in this process do not seem possible at present, nevertheless it is clear from the experimental data that the degree of stabilization of the structure by sugar should be sufficiently great as to affect appreciably the energetic balance between the *Pn*3*m* and *Ia*3*d* cubic phases (Turner et al. 1992; Chung and Caffrey 1994).

Monoolein in anhydrous trehalose platelets

In the lower frame of Fig. 4 the *Pn*3*m* unit cell dimensions measured from the monoolein phase embedded in trehalose platelets are shown as a function of the dehydration time, both for samples dried in the desiccator and in the oven. In both cases the unit cell decreases to very low values ($a = 80$ Å and $a = 70$ Å, when samples are dehydrated for a long time in the desiccator and in the oven, respectively), even less than those observed in concentrated trehalose solutions. Similar dimensions were observed for monoolein in pure water at very high temperatures [for example, $T = 86$ °C, $c_{lip} = 0.74$, $a = 70.8$ Å (Briggs et al. 1996)]. It is noticeable that no differences in the *Pn*3*m* cubic dimensions were observed when the sugar mixture converts to the glassy state ($n_{wat}/n_{tre} < 2$, cf. Fig. 1); no apparent structural modifications are detected that can be related to changes of the viscosity of the medium or to mechanical pressure (Mariani et al. 1997) exerted on the lipid phase after vitrification.

The unit cell variations shown in the lower frame of Fig. 4 can be fitted in terms of exponential behavior. In agreement with calorimetric measurements on trehalose-water binary mixtures, showing that dehydration is faster the higher the temperature, decay constants were obtained of 4.4 ± 0.8 h and 1.5 ± 0.3 h for samples dried in the desiccator and in the oven, respectively. We note that the present dried samples are prepared in a vast trehalose excess (see Materials and methods), and therefore the measured thermodynamic quantities appear essentially determined by trehalose. Moreover, it should be also noticed that X-ray diffraction measurements reported here do reflect reversible equilibrium conditions. In fact the cell parameter measured in a sample dehydrated for some time returns again to the initial value after rehydration, with no apparent hysteresis or dependence on the initial state of the dried platelets.

The lipid concentration of the *Pn*3*m* phase embedded in the trehalose glasses was estimated by solving Eq. (1) using $L_{lip} = 17.3$ Å. As before, it is important to point out that, in the calculations, no assumptions are made about the content of the sugar in the cubic phase. The left, upper frame of Fig. 7 shows the calculated lipid concentration of the cubic phase as a function of the water content of the trehalose platelets. A different behavior characterizes samples dehydrated in the desiccator or in the oven, suggesting that a thermodynamic model, based upon water equilibrium between the lipid phase and the trehalose moiety, cannot explain the results. From the estimated lipid composition, the *Pn*3*m* structural parameters were finally calculated using Eqs. (2), (4), and (5). The results are shown as a function of the water content on the trehalose glasses in the other frames of Fig. 7. It is interesting to compare these data with those obtained in pure water (Fig. 5). De-

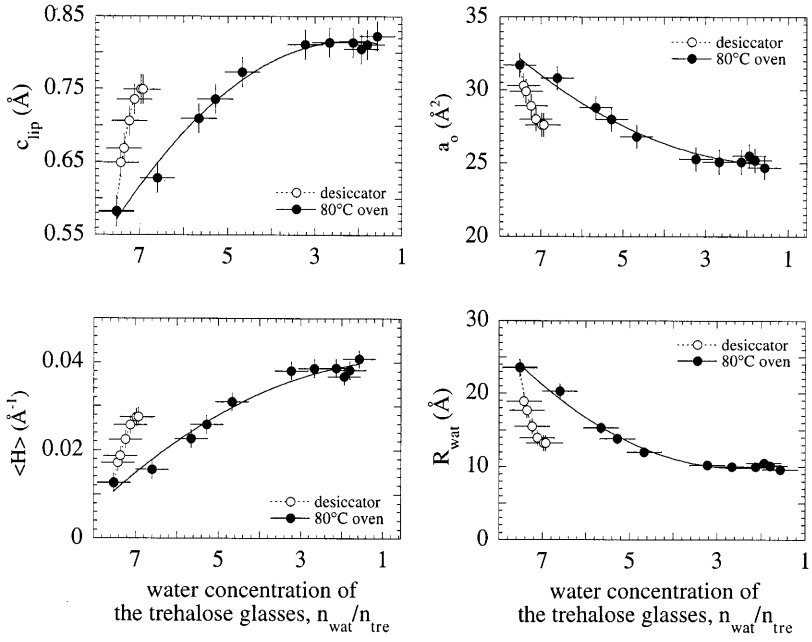

Fig. 7 Variation of the structural parameters of the *Pn*3*m* cubic phase obtained in trehalose platelets as a function of the water-to-trehalose molar ratio in the glasses, n_{wat}/n_{tre}. Data relative to samples dehydrated both in the desiccator and in the 80 °C oven are reported. c_{lip} is the estimated lipid concentration of the cubic phase calculated as reported in the text assuming a constant lipid length for monoolein of 17.3 Å. Other notations and symbols as in the text and in Fig. 5. Lines are visual guides to show the general trend

hydrating the monoolein in trehalose glasses, the lipid uniquely shows the *Pn*3*m* cubic structure. However, the cubic phase presents a highly curved interface and very small areas-per-lipid at the headgroup and very narrow water channels resulted from the calculation. In particular, R_{wat} and a_0 reach values very close to those observed in the *Ia*3*d* cubic phase in pure water, just before the transition to the lamellar phase. Accordingly, the *Pn*3*m* configuration should be highly unstable (Turner et al. 1992; Chung and Caffrey 1994). However, as in concentrated trehalose solutions, the transition to the *Ia*3*d* cubic phase is prevented, confirming that the sugar exercises an additional direct stabilization.

Discussion

The effect of trehalose on the mesomorphic properties of the monoolein-water system dried in the presence of trehalose was studied by X-ray diffraction. While in pure water the *Pn*3*m* and *Ia*3*d* bicontinuous inverse cubic structures and a lamellar Lα phase are observed as a function of concentration, a strong stabilization of the *Pn*3*m* cubic phase has been detected in the presence of trehalose. In concentrated trehalose solutions, but also in trehalose glasses under extremely dry conditions, the *Pn*3*m* cubic unit cell dimension reversibly decreases to very low values, but no evidence of phase transition is seen during dehydration. Assuming that the lipid monolayer thickness is only dependent on temperature (Briggs et al. 1996), the lipid concentration of the *Pn*3*m* cubic phase forming in the presence of trehalose, both in solution and in the vitreous state, has been calculated and the different structural parameters estimated. In particular, the area-per-lipid at the headgroup decreases to very small values, comparable to the one observed on the monoolein monolayer at the air-water interface at the collapse pressure. As briefly reported, the presence of the sugar also affects the temperature of the *Pn*3*m* cubic to hexagonal H_{II} phase transition, strongly confirming that trehalose tends to decrease the area of contact between the lipid and the aqueous phase. Such effects were already observed on other lipid systems, resulting in the stabilization of the normal gel Lβ' phase relative to the interdigitated gel Lβ(i) (Takahashi et al. 1997) or in the formation of a H_{II} phase at the expense of a Lα (Koynova et al. 1989); in such cases, the observed effects were interpreted by the fact that trehalose behaves as a kosmotropic reagent, i.e. as a water-structure-making reagent. The present data show that trehalose strongly affects the structural properties of the *Pn*3*m* cubic phase, resulting in a highly unstable configuration, but no phase transitions occur. Therefore, a simple osmotic mechanism, as observed for example in poly(ethylene glycol) aqueous solutions (Chung and Caffrey 1994), can be excluded. An additional stabilization of the lipid phase, arising from interfacial free energy changes due to trehalose-water-lipid direct interactions, and big enough to affect the energetic balance between the *Pn*3*m* and the *Ia*3*d* cubic phases, should occur.

When the sugar mixture converts to the glassy state, all long-range molecular motions are hindered; however, no changes in the structural properties of the cubic phase are induced by the vitrification mechanism. This observation could have very important biological implications in the biopreservation; in fact, proteins and cell membranes might be expected to be kept in their native states not only by indirect effects due to the stabilization of the water structure, but also direct interactions with sugar, unrelated to the trehalose state, should account for its protectant role in anhydrobiotic organisms.

One last point has to be stressed: the stabilization process hinges upon the trehalose content of the lipid phase,

an experimental parameter that plays a crucial role in the effectiveness of the direct interactions. The very small aqueous channels in the *Pn3m* monoolein phase forming in the presence of trehalose contain the sugar; however, reliable estimates of the sugar concentration in the lipid phase do not seem possible at present, so that the mechanism of the interaction cannot be more deeply investigated.

Acknowledgements We gratefully acknowledge Dr. B. Dubini for performing calorimetric measurements. This work has been co-financed by European Community funds for regional development.

References

Anderson DM, Gruner SM, Leibler S (1988) Geometrical aspects of the frustration in the cubic phases of lyotropic liquid crystals. Proc Natl Acad Sci USA 85: 5364–5368

Briggs J, Caffrey M (1994) The temperature-composition phase diagram of monomyristolein water: equilibrium and metastability aspects. Biophys J 66: 377–381

Briggs J, Chung H, Caffrey M (1996) The temperature-composition phase diagram and mesophase structure characterization of the monoolein/water system. J Phys II (Paris) 6: 723–731

Chung H, Caffrey M (1994) The curvature elastic-energy function of the lipid-water cubic mesophase. Nature 368: 224–226

Cordone L, Galajda P, Vitrano E, Gassmann A, Ostermann A, Parak F (1998) A reduction of protein specific motions in coligated myoglobin embedded in trehalose glass. Eur Biophys J 27: 173–176

Crowe LM, Crowe JH (1988) Trehalose and dry dipalmitoyl phosphatidylcholine revisited. Biochim Biophys Acta 946: 193–201

Crowe JH, Crowe LM, Chapman D (1984) Preservation of membranes in anhydrobiotic organisms: the role of trehalose. Science 223: 701–703

Crowe LM, Crowe JH, Carpenter JF, Wistrom CA (1987) Stabilization of dry phospholipid bilayers and proteins by sugars. Biochem J 242: 1–10

Franks F, Hatley RHM, Mathias SF (1991) Materials science and the production of shelf-stable biologicals. Biopharmacology 4: 38–42

Green JL, Angell CA (1989) Phase relations and vitrification in saccharide-water solutions and trehalose anomaly. J Phys Chem 93: 2880–2882

Gulik A, Luzzati V, De Rosa M, Gambacorta A (1985) Structure and polymorphism of bipolar isoprenyl ether lipids from *Archeabacteria*. J Mol Biol 182: 131–149

Hyde ST, Andersson S, Ericsson B, Larsson K (1984) Z Kristallogr 168: 213–219

Koynova R, Caffrey M (1994) Phases and phase transitions of the hydrated phosphatidylethanolamines. Chem Phys Lipids 62: 253–262

Koynova RD, Technov BG, Quinn PJ (1989) Sugars favour formation of hexagonal (H_{II}) phase at the expense of lamellar liquid-crystalline phase in hydrated phosphatidylethanolamines. Biochim Biophys Acta 980: 377–380

Lide DR (ed) (1996) Handbook of chemistry and physics. CRC Press, Boca Raton

Longley W, McIntosh TJ (1983) A bicontinuous tetrahedral structure in a liquid crystalline lipid. Nature 303: 612–614

Luzzati V, Vargas R, Mariani P, Gulik A, Delacroix H (1993) Cubic phases of lipid-containing systems. Elements of a theory and biological connotations. J Mol Biol 229: 540–551

Mariani P, Luzzati V, Delacroix H (1988) Cubic phases of lipid-containing systems. Structure analysis and biological implications. J Mol Biol 204: 165–189

Mariani P, Paci B, Bosecke P, Ferrero C, Lorenzen M, Caciuffo R (1997) Effects of hydrostatic pressure on the monoolein-water system: an estimate of the energy function of the inverted *Ia3d* cubic phase. Phys Rev E 54: 5840–5843

Sanderson PW, Lis LJ, Quinn PJ, Williams WP (1991) The Hofmeister effect in relation to membrane lipid phase stability. Biochim Biophys Acta 1067: 43–50

Schoen AH (1970) Infinite periodic minimal surfaces without self-intersections. NASA Technical Note TND-5541. NASA, Washington

Scriven LE (1976) Equilibrium bicontinuous structure. Nature 263: 123–125

Takahashi H, Ohmae H, Hatta I (1997) Trehalose-induced destabilization of interdigitated gel phase in dihexadecyl phosphatidyl choline. Biophys J 73: 3030–3038

Tsonev LI, Tihova MG, Brain APR, Yu Z-W, Quinn PJ (1994) The effect of cryoprotective sugar, trehalose, on the phase behaviour of mixed dispersions of dioleyl derivatives of phosphatidylethanolamine and phosphatidylcholine. Liq Cryst 17: 717–728

Turner DC, Wang Z-G, Gruner S, Mannock DA, McElhaney RN (1992) Structural study of the inverted cubic phases of di-dodecylalkyl-β-D-glucopyranosyl-*rac*-glycerol. J Phys II (Paris) 2: 2039–2063